



Nickel sulphide flakes improved cone-shaped graphite electrode for high-performance OER activity

HAYDAR ALI¹, SANTU GHOSH¹ and AVIJIT MONDAL^{2,*} 

¹School of Materials Science, Indian Association for the Cultivation of Science, Kolkata 700032, India

²Department of Chemistry, Presidency University, Kolkata 700073, India

*Author for correspondence (avijit.chem@presiuniv.ac.in)

MS received 16 March 2021; accepted 8 June 2021

Abstract. The performance of electrochemical water splitting is very much affected by the sluggishness of oxygen evolution reaction (OER) process. Therefore, design and development of low cost, stable and active catalyst for OER process is a challenging issue. In this study we have used cone-shaped pencil graphite (PG), which is commonly used for writing purpose, as anode followed by modification by two-dimensional (2D) nickel sulphide flakes for electrochemical OER in alkaline medium. The dispersed flakes gradually attached to the cone-shaped graphite pencil surface via interaction with exposed graphite sheets along with formation of porous network around the electrode surface via assembly of the flakes. The modified electrocatalyst were well characterized using X-ray diffraction, Raman, field emission scanning electron microscopy, energy dispersive X-ray, inductively coupled plasma atomic emission spectroscopy and electrochemical techniques. We have observed that the electrocatalytic activity and stability of the newly designed anode is far greater than standard IrO₂ catalyst-modified PG in alkaline medium and comparable with newly reported Ni-based catalysts modified electrode in literature. The unique shape and porous network facilitate mass diffusion process preventing larger bubble formation. Overall, the approach is very simple and cost effective.

Keywords. Pencil graphite; nickel sulphide; OER; stable; activity.

1. Introduction

Electrochemical water technology is one of the promising ways to produce hydrogen energy to manage worldwide energy demand and reduce carbon emission [1,2]. Water splitting composed of two simultaneous redox reactions, one is 4e⁻ transfer oxidation by anode for O₂ evolution and other is 2e⁻ transfer reduction by cathode for H₂ evolution [1,2]. Researchers are trying to develop catalysts to modify anode and cathode considering four vital issues, these are to increase activity, reduce overpotential, enhance longevity and decrease cost [3–5]. The main function of the catalysts is to generate feasible pathway for increasing the rate of two electrochemical transformation occurring at two electrochemical interfaces. Between these two electrochemical processes, oxygen evolution reaction (OER) is kinetically slow process and hence the design of suitable OER catalyst is more challenging. The solubility of O₂ is greater than H₂ gas in aqueous medium, so O₂ gas in the form of bubble stays longer period of time and joined together to form bigger bubble, which hamper the mass transport/diffusion

process and hence lowers the performance of catalyst [6,7]. Noble metal oxide (RuO₂, IrO₂) is used as standard or control catalyst for OER process, but problem arises for commercialization due to its lack of availability, rapid deactivation and high cost [8,9]. Different non-noble transition metal oxide/hydroxide/sulphide/phosphide/nitride/double-layered hydroxide, etc. were reported in literature and showed good catalytic activity and stability compared to standard catalysts towards OER [1–16]. Nickel sulphides (NiS_x)-based different nanostructures have drawn greater attention in recent years, due to its easy synthesis and good performance for OER process [17]. Some of the related articles are discussed here. Li *et al* [18] designed leaf-like Ni₂S₃ grown on Ni foam by high temperature hydrothermal method, which showed OER activity at 125 mV overpotential (η) to obtain 10 mA cm⁻² current density (j) [18]. NiS_xP_y 1D hybrid nanostructure was formed on Ni foam by high temperature hydrothermal followed by high temperature phosphotization in inert atmosphere, which shows $\eta = 192$ mV at $j = 10$ mA cm⁻² for OER process [19]. The OER activity of Ni₃S₂ in alkaline media was

Supplementary Information: The online version contains supplementary material at <https://doi.org/10.1007/s12034-021-02519-x>.

Published online: 14 August 2021

boosted in the presence of amorphous carbon support, which facilitate electron and mass transfer and overtopping of Fe^{3+} that induce strain in the basic structure to increase activity with $\eta = 350$ mV at $j = 10$ mA cm^{-2} [20]. The mechanistic study also revealed that the thick layer of active species, NiOOH was easily formed on the surface of Ni_3S_2 surface in alkaline media, which is mainly responsible for OER activity [21]. The NiS_x @ graphite was generated through high temperature sulphurization of Ni-metal organic framework followed by high temperature annealing. The catalytic activity was greater compared to RuO_2 or IrO_2 due to large specific surface area, porous structure and conductive support [22]. The high temperature solvothermal synthesis of Ni^{3+} rich hierarchical Ni_3S_4 network revealed good performance, $\eta = 300$ mV at $j = 50$ mA cm^{-2} due to enhanced chemisorption of OH^- in alkaline media and showed no loss of activity after 300 h at 50 mA cm^{-2} [17].

From the above discussion and literature reports, we may say that nickel sulphide-based nanostructures were used as active template for the formation of active species NiOOH, which catalyse OH^- to O_2 formation via electrochemical approach [17,20,21]. However, the synthesis techniques used were either high temperature hydrothermal method or high temperature colloidal heating technique or high temperature furnace heating in inert atmosphere to prepare nickel sulphide-based catalysts. So various methods used for fabrication are not easy and cost effective, and very often costly electrode setup was used. To overcome these issues, we have developed a simple and cost-effective strategy to modify cone-shaped PG by nickel sulphide template using the interaction between 2D nickel sulphide flakes and exposed graphite surface sheets. In the presence of alkaline environment, the surface of NiS_2 gradually changes to hydrated complex of Ni^{2+} . This nickel-based catalyst shows $\eta = 300$ mV at $j = 20$ mA cm^{-2} current density for OER process. This electrode has several advantages, such as, (a) does not require any surfactant, (b) commercially available electrode material and chemicals, (c) *in-situ* electrode fabrication at room temperature, (d) no large bubble formation problem due to its shape and surface morphology, (e) stable for long time use, etc.

This simple technology is not reported yet in literature as per our best of knowledge to obtain low cost, stable anode for OER process and used in three electrode-based system, where the commercial Pt wire is used as counter electrode and saturated Ag/AgCl as a reference electrode.

2. Experimental

2.1 Materials

Nickel(II) chloride hexahydrate, nafion perfluorinated resin solution (5 wt%), potassium hydroxide, sodium sulphide,

iridium(IV) oxide are purchased from Sigma Aldrich. Graphitic pencil is purchased from normal shop.

2.2 Instrumentation

The deposited films of catalyst were measured by the X-ray diffraction (XRD) analysis using $\text{Cu-K}\alpha$ X-ray ($\lambda = 1.5418$ Å) radiation in a Seifert 3000P Bragg diffraction set up. The field emission scanning electron microscopy (FE-SEM) analysis and elemental diffraction X-ray analysis were performed with Supra 40, Carl Zeiss Pvt. Ltd. Instrument. Raman spectra were taken on a J-Y Horiba confocal triple Raman spectrometer (model: T64000) with a 532 nm excitation Nd:YAG laser (Spectra Physics). The exact amount of catalyst loaded on electrode surface was quantified by an Optima 2100DV inductively coupled plasma atomic emission spectroscopy (ICP-AES, PerkinElmer).

2.3 Preparation of nickel sulphide modified cone-shaped electrode

The pencils were sharpened at both sides with a fixed length using a normal sharpener (same for all) until a cone shape is formed. One side was used for electrode modification and the other side was used for attachment with current collector. The cone-shaped pencils are washed using ethanol-water mixture through sonication to remove loosely bound graphitic particles and used for further modification. Next, 500 μl NiCl_2 (0.1 M) and 50 μl nafion solution (0.5 wt%) were mixed thoroughly. After that, 150 μl Na_2S solution (1 M) was added quickly and vortexed for 20 min to mix well. The colour of solution changes from colourless to black. The cone-shaped pencil was dipped into the black solution for overnight. Dipped portion of the pencil was then washed with water several times followed by air-drying. These cones-shaped electrodes were measured at a fixed length (7 mm) and radius (1.1 mm) using Vernier calipers so that all pencils have same surface area and rest portion of the pencil was coated with Teflon tape not to expose to electrochemical activity. These Teflon-coated cone-shaped modified electrodes were used for electrochemical study. For control experiment, 3 mg of IrO_2 was dispersed in 270 μl double-distilled water with 30 μl 0.5 wt% nafion via ultrasonication for 20 min. Then 30 μl of IrO_2 was dropcasted on cone-shaped pencil graphite (PG) carefully so that required surface area covered by standard catalyst slurry and dried at room temperature.

2.4 Electrochemical characterization

A Teflon-coated cone-shaped pencil with a fixed surface area of 0.2448 cm^2 was used for all electrochemical studies, and details of calculation are shown in supplementary

figure S1. Electrochemical measurements were done with a CHI633D electrochemical analyser in a conventional three-electrode system, which was made out of an Ag/AgCl/saturated KCl as a reference electrode, a platinum wire as an auxiliary electrode and a modified Teflon-coated pencil as a working electrode. Three-electrode system with current collector is shown in supplementary figure S2. Every single electrochemical examination was performed at room temperature. For OER, the cyclic voltammograms (CV), linear sweep voltammograms (LSV) were recorded at a scan rate of 2 mV s^{-1} and amperometric *i-t* study was performed at 1.52 V (vs. reversible hydrogen electrode (RHE)) in 1 M KOH . The continuous CV cycle at a time (for 500 and 1000 CV cycles) was done at a scan rate 50 mV s^{-1} . All the potentials were reported with respect to RHE using expression, $E_{\text{RHE}} = 0.197 + E_{\text{Ag/AgCl}} + 0.059 \text{ pH}$. Electrochemical impedance spectroscopy (EIS) was recorded in a frequency range of 0.1 Hz – 10 kHz with a sinusoidal voltage amplitude of 5.0 mV at bias potentials of -0.2 and 1.52 V (vs. RHE) for the OER using Biologic SP300 electrochemical workstation. The CVs were measured in the potential range 1.1 – 1.2 V (vs. RHE) at various scan rates (5 – 80 mV s^{-1}). $\Delta J/2$ vs. scan rate was plotted to obtain double layer capacitance (C_{dl}), where $\Delta J = j_a - j_c$. All CV and LSV plots were *iR* corrected.

3. Results and discussion

Every colloidal solution has tendency to precipitate out of the solution by forming large particle with time and hence we used this concept to modify graphite pencil for anode. The colloidal solution of nickel sulphide formed larger precipitate with time at the bottom of the container along with attachment of small amount of nickel sulphide flakes strongly on the rough graphite surfaces of the cone-shaped pencil. The exposed graphite sheets may help firm attachment through hydrophobic/metal ion- π ring interaction [23,24]. Nafion polymer acts as binder as well as support for nickel sulfide sheets, which helps to directly attach to the cone-shaped graphite electrode surface for *in-situ*

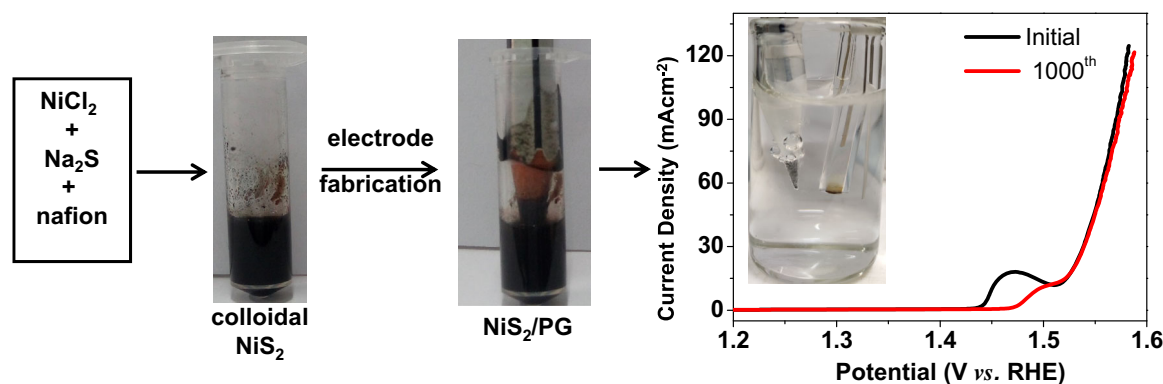
preparation and we did not require any external surfactants. The synthetic approach along with electrochemical performance is shown in scheme 1.

Initially tiny flakes are attached to the solid support followed by the formation of larger 2D flakes on the entire dipped portion of the pencil surface. These flakes did not detach from the surface after repeated and thorough washing by water, which signifies that these are strongly grafted on the solid support.

The PG and nickel sulphide flakes were systematically characterized via different techniques. In figure 1a, the XRD pattern of PG is due to reflection of (002), (004) graphitic planes. The observed different reflections from various planes of nickel sulphide closely matches with cubic structure of NiS_2 (JCPDS file no.800375) than any other structure of nickel-based sulphide crystals.

The four main reflections from (111), (200), (220) and (222) planes are shown in figure 1a, which exactly matches with standard spectra. However, other peaks are not clearly observed from the data. The existence of nafion polymer in the reaction mixture may cover some specific planes. We have also studied XRD after keeping initially formed NiS_2 in alkaline environment for different period of time (0, 2, 5 and 7 h) to get information about surface structure. However, the XRD pattern of NiS_2 gradually changes due to the formation of crystal $\text{K}_2\text{Ni}(\text{SO}_4)_2 \cdot 6\text{H}_2\text{O}$ in the presence of 1 M KOH solution, which is shown in supplementary figure S3. The XRD pattern of NiS_2 at 2 h matches with the mentioned crystal system with JCPDS no. 13-0193. After 5 and 7 h, the intensity of different reflections increases along with intensity for the reflections due to gradual transformation of NiS_2 surface. The XRD characterization implies that NiS_2 may be in precatalytic state to show catalytic activity. Graphitic signature of pencil electrode is observed by Raman spectra, in figure 1b, with I_D/I_G ratio of 0.45. The ratio is increased to 0.64 after modification of GP by NiS_2 sample, which reflects increment of defect state in graphitic structure due to strong attachment of nickel flakes on graphitic surface.

The FE-SEM images showed two-dimensional flakes of nanometre in width and micrometre length grown on PG



Scheme 1. Schematic representation of NiS_2 formation on PG electrode along with OER performance.

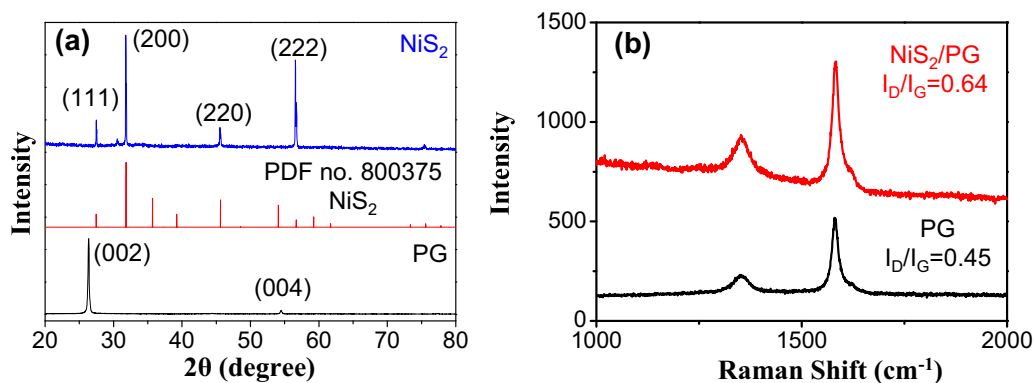


Figure 1. (a) X-ray diffraction pattern of graphite pencil and NiS₂. (b) Raman signal of graphitic nature of pencil graphite before and after modification of NiS₂.

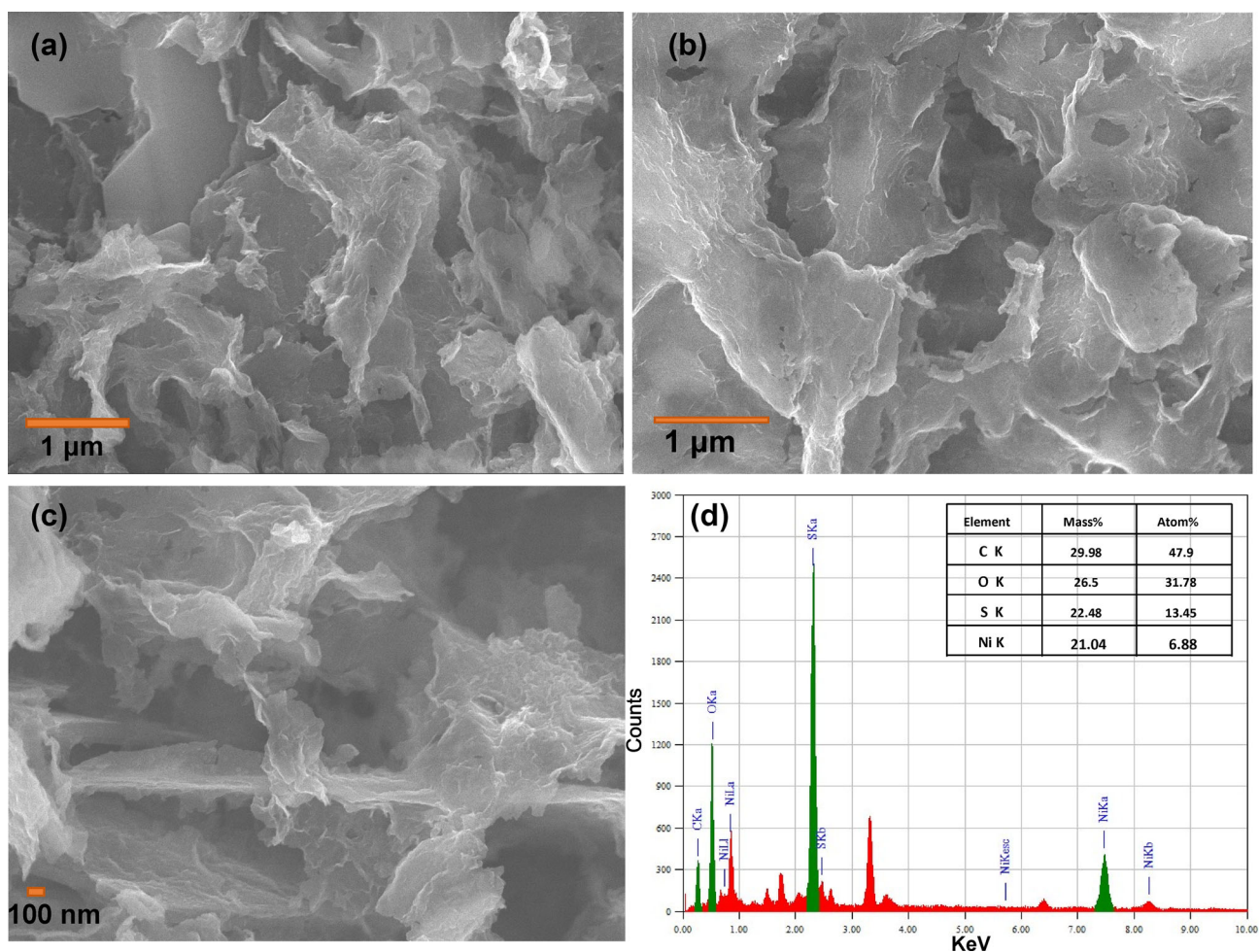


Figure 2. (a–c) FE-SEM images at different magnifications of 2D NiS₂ flakes. (d) Elemental diffraction X-ray analysis for different elements present on electrode with atomic and mass percentage.

from a colloidal solution of NiS₂, which is shown in figure 2a–c. These flakes are arranged in such a way that porous network form throughout the electrode surface, which will provide greater surface area towards electrolyte and increase the rate of mass transfer during electrochemical study. Elemental signature is obtained through EDX

analysis along with atomic and mass percentage ratio, as shown in figure 2d. The atomic percentage ratio of nickel to sulphur element is approximately equal to 0.5, which also support XRD study for NiS₂ formation.

By linear sweep voltammetry study, the designed electrode showed higher catalytic activity (shown in figure 3a)

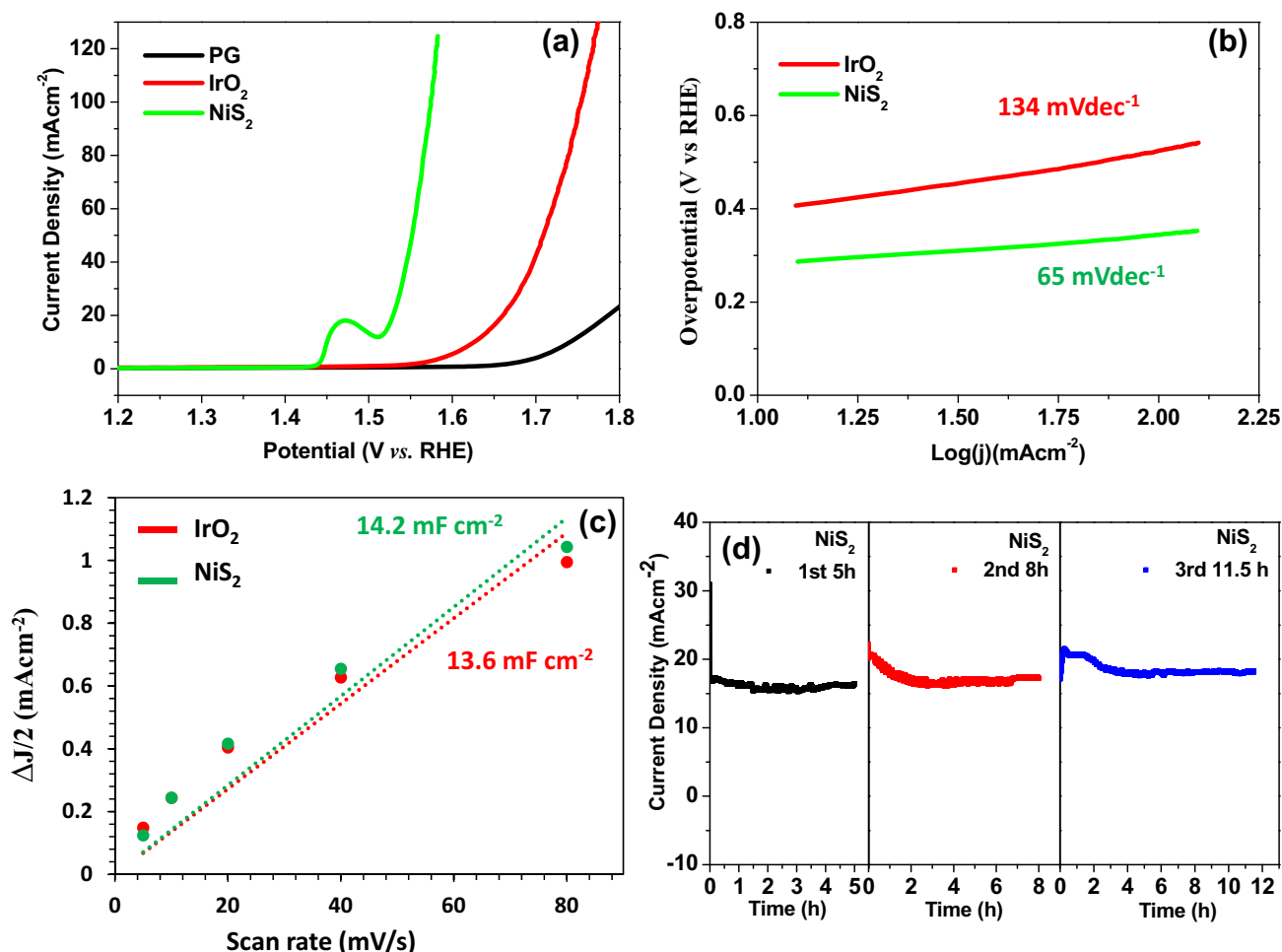


Figure 3. (a) Linear sweep voltammograms at scan rate 2 mV s⁻¹. (b) Tafel plot for IrO₂ and NiS₂ modified electrodes. (c) C_{dl} value measurement from the plot ΔJ/2 at 1.15 V (vs. RHE) vs. scan rate. (d) Stability testing of NiS₂ modified electrode via amperometric i-t curve technique at 1.52 V vs. RHE using three round study. All the measurements were done in 1 M KOH.

compared with standard control IrO₂ modified electrode and pure PG electrode. The broad characteristic peak was observed around in the range 1.43 to 1.53 V due to oxidation of Ni²⁺ to active Ni³⁺ and followed by oxidation of OH⁻ to O₂ by active Ni³⁺ formed on the surface of the catalyst. The observed overpotential (η) for OER process is 300 mV at $j = 20 \text{ mA cm}^{-2}$ for NiS₂, whereas for IrO₂-modified anode, η is 429 mV at $j = 20 \text{ mA cm}^{-2}$. So smaller overpotential was observed for NiS₂ compared to IrO₂, which signifies that the catalytic activity of NiS₂ is far better compared to IrO₂. The catalytic activity of control IrO₂ is quite reasonable at higher potential range, and there were similar types of catalytic activity of IrO₂ reported in literature [23,25,26]. The OER activity for pure PG is very less with $\eta = 558 \text{ mV}$ at $j = 20 \text{ mA cm}^{-2}$. Comparative performances of reported material with our designed material for OER process is given in supplementary table S1. The Tafel slope (figure 3b) of NiS₂ (65 mV dec⁻¹) shows a much lower value compared to IrO₂ (134 mV dec⁻¹), which reflects the faster electrode reaction that takes place on NiS₂ surface. Electrochemical surface area (ECSA = C_{dl}/C_s,

C_s = capacitance of the electrolyte) is directly proportional to the double layer capacitance (C_{dl}) of the double layer formed on the electrode–electrolyte interface in non-faradic region. C_{dl} were measured from the slope of the plot ΔJ/2 at 1.15 V vs. scan rate (figure 3c and supplementary figure S4) [10,19,27,28]. The calculated ECSA are 86.9 (NiS₂) and 83.2 cm² (IrO₂), considering the specific capacitance value of 0.040 mF cm⁻² in 1 M KOH [29] (for ECSA calculation, see supplementary information). Initially C_{dl} value for NiS₂ is comparable with IrO₂ electrode, as observed from figure 3c, though the activity of NiS₂ is much higher compared to standard IrO₂. Gradually C_{dl} value increased with time, as shown in figure 4. The specific activity is measured using ECSA and the NiS₂ catalyst has 28.3 times greater specific activity than IrO₂ at $\eta = 340 \text{ mV}$ (table 1 and supplementary figure S5). We have tested the stability of NiS₂ through amperometric i-t study for different time period, which shows that the nickel-based catalyst is highly stable in nature and activity is increasing with time for 3 different time periods at 1.52 V vs. RHE applied potential (figure 3d). The catalytic activity of the catalyst increases

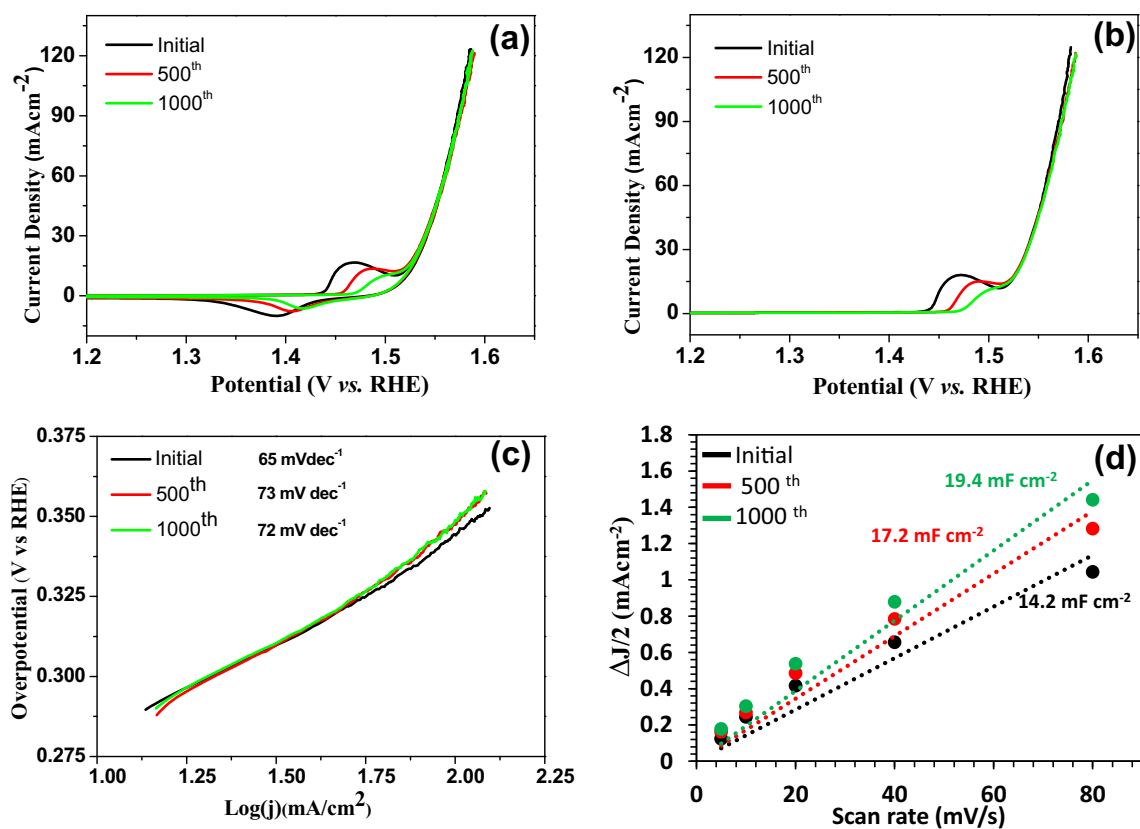


Figure 4. (a) Comparative cyclic voltammetry study for NiS₂ on PG electrode of initial, 500th and 1000th CV cycle at 2 mV s⁻¹ scan rates. (b) Corresponding linear sweep voltammograms at 2 mV s⁻¹. (c) Tafel plot for different scans of LSV studies and (d) C_{dl} measurement from ΔJ/2 at 1.15 V vs. scan rate plot. CV and LSV were done in 1 M KOH.

Table 1. Comparison of OER activity study between NiS₂/PG and IrO₂/PG.

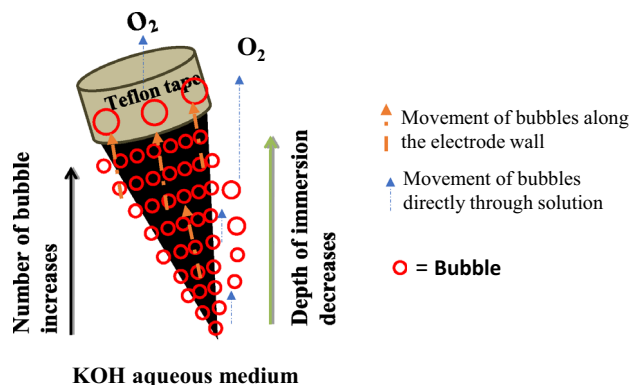
Sample	η (mV) at $j = 20 \text{ mA cm}^{-2}$	Specific activity (Am ⁻²) at $\eta = 340 \text{ mV}$	Mass activity (mA mg ⁻¹) at $\eta = 340 \text{ mV}$	TOF (s ⁻¹)
IrO ₂	448	0.09	2.73	0.7×10^{-2}
NiS ₂	300	2.54	132	1.9×10^{-2}

by little amount from 1st to 2nd to 3rd round study, shown in figure 4. The sample loading on PG for NiS₂ was 0.17 mg, measured by ICP-AES technique and IrO₂ loading on PG was 0.3 mg, calculated manually. The amounts of NiS₂ and IrO₂ present on electrode per cm⁻² were 0.695 and 1.225 mg cm⁻², respectively. The mass activity of NiS₂/PG anode is 48.3 times greater than IrO₂/PG anode (table 1 and supplementary figure S5). Also, we have calculated the turn over frequency (TOF) at $\eta = 340 \text{ mV}$ for NiS₂ and IrO₂, i.e., 1.9×10^{-2} and $0.7 \times 10^{-2} \text{ s}^{-1}$, respectively (table 1, supplementary information) [10,30].

The peak area due to oxidation of Ni²⁺ to Ni³⁺ in forward scan and the peak area for reduction of Ni³⁺ to Ni²⁺ in reverse scan from initial to 1000th CV cycle decreases keeping OER activity almost unchanged in current density. The peak position changes with increasing number of scans (figure 4a) [31–33].

There may be partial irreversible oxidation of Ni²⁺ to NiO_x/Ni(OH)_x, which is responsible for lowering peak areas. Similar type of lowering in the peak area was observed in the case of α -Ni(OH)₂ reported by Luan and co-workers [10]. These species formed from original catalyst NiS₂ during ongoing scan are active in nature to keep activity steady [34]. The activity of IrO₂-modified electrode decreases after 100 CV cycles considerably (supplementary figure S6). More clear data are observed from the LSV study, which shows that peak maxima for oxidation of Ni²⁺ to Ni³⁺ shifts to higher potential with decreasing peak area (figure 4b). This type of phenomenon can be explained using Tafel slope and C_{dl} measurement (figure 4c and d, and supplementary figure S7). The Tafel slope increased with repeated CV scans, values are mentioned in figure 4c, which reflects little lowering of reaction kinetics compared to the initial electrode reaction. However, the OER activity

remains almost same due to enhancement of ECSA, which is directly related to increase in C_{dl} value, observed from figure 4d, with number of CV cycles. This C_{dl} value increment may explain the little enhancement of current density in amperometric i-t study also. Initially Ni^{2+} is in an environment of sulphide mostly and with repeated scan in 1 M KOH, oxide/hydroxide/oxyhydroxide nature around metal ions increases due to nucleophilic attack of OH^- ,



Scheme 2. Schematic representation of bubble formation on cone-shaped surface and liberation of O_2 .

which diminishes sulphide nature of the catalyst [17,35,36]. The EDX analysis data of the catalyst after 1000 CV cycles (supplementary figure S8) clearly shows that nickel to sulphur element ratio increased from 0.5 (figure 2d) to 7, and support this type of environment change of active catalyst. This type of change in environment can also be easily understood from gradual increment in Tafel slope, and ECSA area increases due to rupture of the large 2D network through nucleophilic attack of OH^- to generate smaller 2D network (supplementary figure S8). In addition, from XRD study of NiS_2 in the presence of KOH shows Ni^{2+} easily form complex with water molecules in alkaline media, which may possibly help for the formation of active $NiOOH$ species.

The small 2D network with more porous nature is observed in FE-SEM study of the catalyst after 1000 CV cycles also and these may lead to increase of surface area. There are many reports that the nickel-based catalyst shows good performance towards OER is due to presence of Fe^{3+} in KOH as impurity [14,37,38]. Therefore, there may be a possibility of catalytic effect of Fe^{3+} ions and we will focus on this issue in our next work.

The unique cone-shaped geometry and porous 2D flakes provide easy gas diffusion process and prevent larger bubble formation around the electrode. The advantage of this

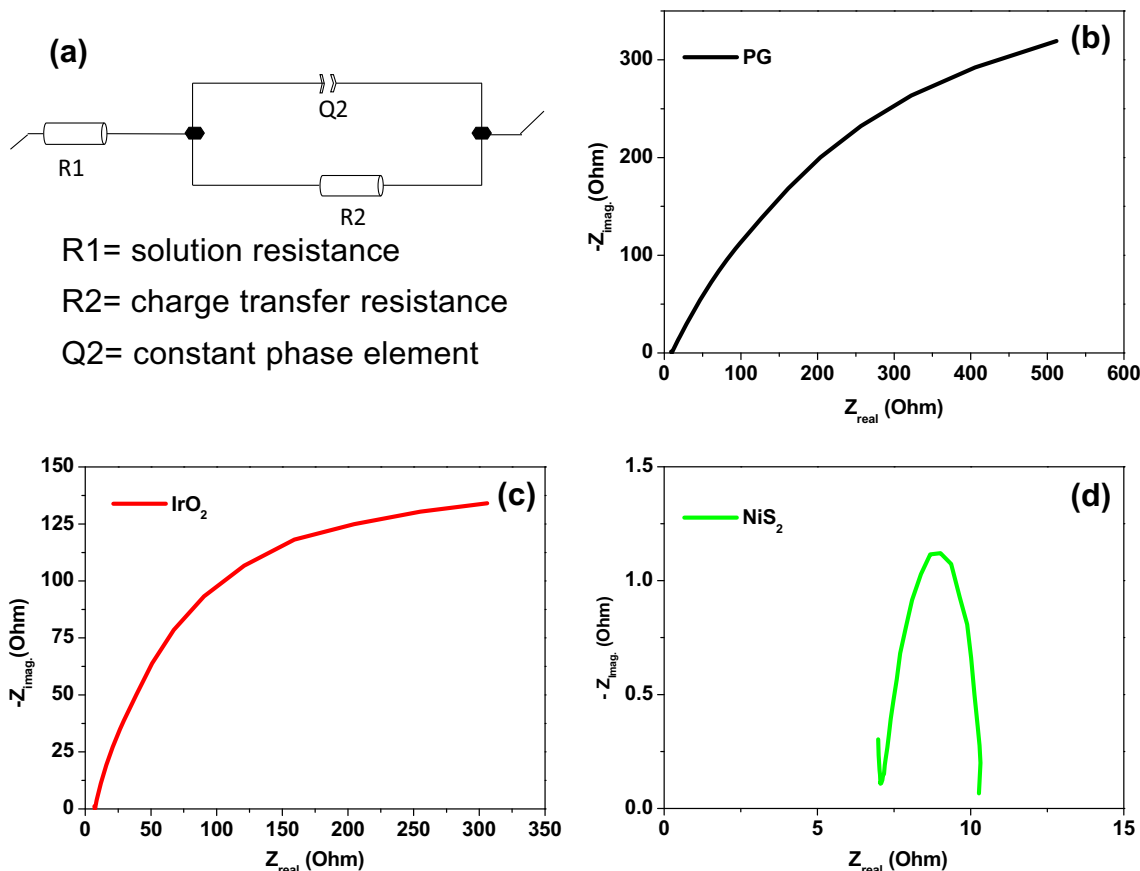


Figure 5. (a) Circuit diagram for Nyquist plot for different electrodes: (b) pure pencil graphite (PG), (c) IrO_2 and (d) NiS_2 .

particular shape of electrode can be realized from the following schematic diagram, which describe probable mechanistic pathway for smaller size bubble formation and release from aqueous medium (scheme 2). The geometric surface area gradually decreases towards tip with depth of immersion increases and consequently the number of bubble formation due to OER also decreases. Also, the electrode was kept at an angle with vertical axis not completely in perpendicular fashion. Therefore, the bubbles formed near the tip region or lower part of the electrode is in a state of greater pressure difference compared to upper part. Consequently, the bubbles at the tip region moves upward directly through the solution as the electrode was kept at somewhat tilt fashion and some bubbles move along electrode wall. The bubbles that move along the wall definitely apply some forces on the bubbles next to it in upward direction and they combine and ultimately form larger bubbles at Teflon-coated surfaces. Hence, the size of the bubbles is not growing very much at the active portion of the electrode due to this typical shape of the electrode compared to commonly used graphite rod (cylindrical shape) or circular-shaped electrode. We have taken a video clip (supplementary Video S1) of a CV cycle in the range 0 to 1.6 V vs. Ag/AgCl at 50 mV s⁻¹ scan rate, which clearly shows no bigger bubble formation in the active region of NiS₂-modified PG electrode during electrolysis. The O₂ gas evolution process is more or less similar to H₂ evolution at Pt wire cathode and we have taken long-range potential to see evolution process for longer period.

Nyquist plots of the electrochemical impedance spectroscopic study show that NiS₂ catalyst on PG has much smaller charge transfer resistance compared to IrO₂ on PG and pure PG electrodes, which clearly indicates that NiS₂ nanosheets strongly grafted on cone-shaped PG electrode and easily transfer charge to the electrode (figure 5). The calculated charge transfer resistance (R_{ct} or R_2) for NiS₂/PG, IrO₂/PG and PG are 3.5, 400 and 1400 ohm. The semicircle nature NiS₂/PG electrode is far better compared to other two electrodes, suggesting higher charge transport efficiency of NiS₂ flakes. This plot also supports NiS₂ as good electrocatalyst for OER activity in an alkaline environment.

4. Conclusion

We have designed cost-effective, active electrode through a most simple process, which shows good activity in 1 M KOH electrolyte for OER process with reasonably lower overpotential. The unique properties of electrode, like unique cone shape, simple colloidal technique for direct electrode modification and porous network by 2D flakes, provide more active surface area along with prevention of bigger bubble formation, keeping the diffusion process very smooth. We will try to investigate the effect of Fe³⁺ ions on

catalytic activity and improve OER performance further by using mixed metal ions (Fe³⁺ and Ni²⁺) as precursors.

Acknowledgements

AM would like to thank the Presidency University and Indian Association for the Cultivation of Science (IACS) for providing research facilities. HA and SG acknowledge DST, India, for providing research fellowship.

References

- [1] Jiao Y, Zheng Y, Jaroniec M and Qiao S Z 2015 *Chem. Soc. Rev.* **44** 2060
- [2] Roger I, Shipman M A and Symes M D 2017 *Nat. Rev.* **1** 1
- [3] You B and Sun Y 2018 *Acc. Chem. Res.* **51** 1571
- [4] Hou J, Wu Y, Zhang B, Cao S, Li Z and Sun L 2019 *Adv. Funct. Mater.* **29** 1808367
- [5] Hu C, Zhang L and Gong J 2019 *Energy Environ. Sci.* **12** 2620
- [6] Atkins P and de Paula J 2009 *Physical chemistry* 9th edn (Oxford: W H Freeman)
- [7] Castellan G W 1983 *Physical chemistry* (3rd edn) Addison-Wesley Publishing Company, Inc.
- [8] Lee Y, Suntivich J, May K J, Perry E E and Shao-Horn Y 2012 *J. Phys. Chem. Lett.* **3** 399
- [9] Pfeifer V, Jones T E, Vélez J J V, Arrigo R, Piccinin S, Hävecker M *et al* 2017 *Chem. Sci.* **8** 2143
- [10] Luan C, Liu G, Liu Y, Yu L, Wang Y, Xiao Y *et al* 2018 *ACS Nano* **12** 3875
- [11] Shen L, Yu L, Wu H B, Yu X Y, Zhang X and Lou X W 2015 *Nat. Commun.* **6** 6694
- [12] Zhang C, Shao M, Zhou L, Li Z, Xiao K and Wei M 2016 *ACS Appl. Mater. Interfaces* **8** 33697
- [13] Wu T, Zhang S, Bu K, Zhao W, Bi Q, Lin T *et al* 2019 *J. Mater. Chem. A* **7** 22063
- [14] Dutta A, Samantara A K, Dutta S K, Jena B K and Pradhan N 2016 *ACS Energy Lett.* **1** 169
- [15] Dutta S, Indra A, Feng Y, Han H and Song T 2019 *Appl. Catal. B-Envs.* **241** 521
- [16] Tiwari A P, Yoon Y, Novak T G, An K S and Jeon S 2019 *ACS Appl. Nano Mater.* **2** 5061
- [17] Wan K, Luo J, Zhou C, Zhang T, Arbiol J, Lu X *et al* 2019 *Adv. Funct. Mater.* **29** 1900315
- [18] Li Y, Bu Y, Chen X, Zhu T, Wang J, Kawi S *et al* 2019 *Chem. Cat. Chem.* **11** 1320
- [19] Fu H Q, Zhang L, Wang C W, Zheng L R, Liu P F and Yang H G 2018 *ACS Energy Lett.* **3** 2021
- [20] Han C, Li W, Shu C, Guo H, Liu H, Dou S *et al* 2019 *ACS Appl. Energy Mater.* **2** 5363
- [21] Zheng X, Han X, Zhang Y, Wang J, Zhong C, Deng Y *et al* 2019 *Nanoscale* **11** 5646
- [22] Ma M, Yang G, Wang H, Lu Y, Zhang B, Cao X *et al* 2019 *Int. J. Hydrogen Energy* **44** 1544
- [23] Jothi P R, Salunkhe R R, Pramanik M, Kannan S and Yamauchi Y 2016 *RSC Adv.* **6** 21246
- [24] Krishnamoorthy D and Prakasam A 2020 *Inorg. Chem. Commun.* **119** 108063

- [25] Dai Z, Geng H, Wang J, Luo Y, Li B, Zong Y *et al* 2017 *ACS Nano* **11** 11031
- [26] Liu D, Du Y, Li T, Zhang H, Liu D, Zhang W *et al* 2020 *Chem. Commun.* **56** 11465
- [27] Trasatti S and Petrii O A 1991 *Pure Appl. Chem.* **63** 711
- [28] McCrory C C L, Jung S, Peters J C and Jaramillo T F 2013 *J. Am. Chem. Soc.* **135** 16977
- [29] Sun X, Shao Q, Pi Y, Guo J and Huang X 2017 *J. Mater. Chem. A* **5** 7769
- [30] Gao M, Sheng W, Zhuang Z, Fang Q, Gu S, Jiang J *et al* 2014 *J. Am. Chem. Soc.* **136** 7077
- [31] Thangasamy P, Maruthapandian V, Saraswathy V and Sathish M 2017 *Sci. Technol.* **7** 3591
- [32] Chen J S, Ren J, Shalom M, Fellingner T and Antonietti M 2016 *ACS Appl. Mater. Interfaces* **8** 5509
- [33] Wu L K, Wu W Y, Xia J, Cao H Z, Hou G Y, Tang Y P *et al* 2017 *J. Mater. Chem. A* **5** 10669
- [34] Stern L A and Hu X 2015 *Faraday Discuss.* **176** 363
- [35] Wang H Y, Hsu Y Y, Chen R, Chan T S, Chen H M and Liu B 2015 *Adv. Energy Mater.* **5** 1500091
- [36] Tahir M, Pan L, Zhang R, Wang Y C, Shen G, Aslam I *et al* 2017 *ACS Energy Lett.* **2** 2177
- [37] Trtochaud L, Young L S, Ranney J K and Boettcher S W 2014 *J. Am. Chem. Soc.* **136** 6744
- [38] Michael J D, Demeter E L, Illes S M, Fan Q, Boes J R and Kitchin J R 2015 *J. Phys. Chem. C* **119** 11475